IMA Journal of Numerical Analysis Advance Access published March 24, 2010

IMA Journal of Numerical Analysis Page 1 of 17
doi:10.1093/imanum/drp052

Convergence of de Boor's algorithm for the generation of equidistributing meshes

X. XU†
Department of Mathematics, Simon Fraser University, Burnaby, British Columbia V5A 1S6, Canada

W. HUANG‡
Department of Mathematics, The University of Kansas, Lawrence, KS 66045, USA

R. D. RUSSELL§ AND J. F. WILLIAMS¶
Department of Mathematics, Simon Fraser University, Burnaby, British Columbia V5A 1S6, Canada

[Received on 4 December 2008; revised on 20 November 2009]

A commonly used algorithm for generating adaptive meshes for a given adaptation function in one dimension is due to de Boor. In its original form the algorithm produces a sequence of meshes upon using piecewise constant interpolation for the adaptation function on the current mesh and generating a new mesh that exactly equidistributes the interpolant. In this paper we present a proof for the existence of a limit mesh and for the convergence of de Boor's algorithm. Numerical results are given to illustrate the theoretical findings, and stopping criteria necessary for the implementation of the algorithm are examined.

Keywords: convergence; de Boor's algorithm; equidistributing mesh; mesh adaptation.

1. Introduction

The concept of equidistribution (de Boor, 1973; Burchard, 1974) is perhaps the most fundamental idea in the field of adaptive mesh generation. In one dimension the idea is quite straightforward. If one chooses a so-called adaptation function $\rho(x)$ that in some way indicates the error in the numerical approximation, then, for a given positive integer N, equidistribution entails finding a mesh $\hat{X}$: $a = \hat{x}_0 < \hat{x}_1 < \cdots < \hat{x}_N = b$ such that

$$\int_a^{\hat{x}_i} \rho(x)\mathrm{d}x = \frac{i}{N}\sigma, \quad i = 1, \ldots, N, \tag{1.1}$$

where

$$\sigma = \int_a^b \rho(x)\mathrm{d}x. \tag{1.2}$$

†Email: xux@alumni.sfu.ca. Present address: Department of Mathematics and Physics, China University of Petroleum-Beijing, 18 Fuxue Road, Changping, Beijing 102249, China.
‡Corresponding author. Email: huang@math.ku.edu
§Email: rdr@cs.sfu.ca
¶Email: jfw@math.sfu.ca

Such a mesh is often referred to as an equidistributing mesh since it evenly distributes $\rho(x)$ among its cells. The existence and uniqueness of an equidistributing mesh are guaranteed theoretically when a strictly positive adaptation function is used. (In this case the right-hand side of (1.1) is a strictly increasing function of $\hat{x}_i$ and then the existence and uniqueness of $\hat{x}_i$ follow.) However, it can rarely be found exactly in practice because the integrals in (1.1) must normally be approximated. Thus, one has to rely on numerical methods for finding approximations to the equidistributing mesh even when $\rho(x)$ is known explicitly, not to mention the fact that, in general, $\rho(x)$ depends on solving for the numerical solution together with the mesh. A number of methods have been developed in the past for generating equidistributing meshes. They are typically iterative due to the highly nonlinear nature of the equidistribution relation (1.1). Examples include de Boor's algorithm (de Boor, 1974), where a sequence of meshes is generated to exactly equidistribute a sequence of piecewise constant approximations to the adaptation function, and the so-called moving mesh PDE method (Huang *et al*., 1994), where the approximate equidistributing mesh is obtained by integrating a parabolic differential equation. Newton's iteration has also been used by some researchers (see, e.g., White (1979) and Linss (2001)).

In the past there has been a strong interest in equidistributing meshes. Studies can be traced back to the early works Rice (1969), Dodson (1972), de Boor (1973), Burchard (1974), de Boor (1974) and Russell & Christiansen (1978) on best approximations with variable knots, Sacks & Ylvisaker (1966, 1968, 1970) on regression problems in statistics and Pereyra & Sewell (1975), Babuška & Rheinboldt (1978) and White (1979) on the numerical solution of differential equations. Recent works include Mackenzie (1999), Qiu & Sloan (1999), Beckett & Mackenzie (2000, 2001), Qiu *et al*. (2000), Kopteva & Stynes (2001), Huang & Sun (2003), Huang (2005) and Chen *et al*. (2007). The focus of these studies was the error analysis of equidistributing meshes. This is not surprising since it is important to understand how good an approximation or a numerical solution can be on an equidistributing mesh. What is surprising is that, despite their widespread use, little work has been done in analysing the convergence of the algorithms developed for computing equidistributing meshes. This may partly be attributed to the fact that the high nonlinearity of equidistribution makes its rigourous analysis (and, indeed, that for most adaptive techniques) extremely difficult. But, at the same time, the issue appears to have been largely forgotten (Pryce, 1989). In his innovative work Pryce (1989) considered a modified de Boor's algorithm that uses piecewise linear interpolation for generating equidistributing meshes for a given adaptation function. Given the continuity of piecewise linear interpolation, he was able to prove the existence of the limit mesh as well as the convergence of the algorithm. However, Pryce also observed in numerical experiments that the modified algorithm generally converges slower than the original one (which uses piecewise constant interpolation for approximating the adaptation function) and the nodes of the resulting mesh have a tendency to oscillate in and out of singular layers. Related issues were considered by Kopteva and Stynes (2001) for an upwind finite-difference solution to a singularly perturbed two-point boundary-value problem. For the special case of an arc-length adaptation function they showed the existence of equidistributing meshes and the convergence of de Boor's algorithm when assuming the continuity of the finite-difference solution as a function of the mesh. Their analysis makes use of the special properties of the upwind finite-difference solution and the solution to the underlying differential equation, making it difficult to see how the argument would generalize to other problems.

In this paper we are concerned with the convergence of de Boor's algorithm for a general continuous adaptation function $\rho = \rho(x)$. Assume that ρ has been chosen such that

$$\rho_- \leqslant \rho(x) \leqslant \rho_+ \quad \forall\, x \in [a, b], \tag{1.3}$$

where ρ_- and ρ_+ are positive constants. Given an initial mesh of N elements, $X^{(0)}$, de Boor's algorithm generates a sequence of meshes of N elements by

$$X^{(k+1)} = G_N(X^{(k)}), \quad k = 0, 1, \ldots, \tag{1.4}$$

where the mapping G_N consists of the following two steps.

(a) Compute the piecewise constant interpolant $\bar{\rho}_{X^{(k)}}$ for ρ on the mesh $X^{(k)}$. (See (2.3) below for the definition of the piecewise constant interpolation.)
(b) Compute the new mesh $X^{(k+1)}$ that exactly equidistributes $\bar{\rho}_{X^{(k)}}$ as follows:

$$\int_a^{x_i^{(k+1)}} \bar{\rho}_{X^{(k)}} \,\mathrm{d}x = \frac{i}{N} \int_a^b \bar{\rho}_{X^{(k)}} \,\mathrm{d}x, \quad i = 0, 1, \ldots, N. \tag{1.5}$$

In step (b), $X^{(k+1)}$ can be efficiently computed since the left-hand side of (1.5) defines a piecewise linear function of $x_i^{(k+1)}$ and the integral on the right-hand side can be computed (cf. (2.3) below) as follows:

$$\int_a^b \bar{\rho}_{X^{(k)}} \,\mathrm{d}x = \frac{1}{2} \sum_{i=1}^{N} (x_i^{(k)} - x_{i-1}^{(k)})(\rho(x_{i-1}^{(k)}) + \rho(x_i^{(k)})).$$

Moreover, it is not difficult to see that, when $\{X^{(k)}\}$ converges, the limit mesh X satisfies

$$\int_a^{x_i} \bar{\rho}_X \,\mathrm{d}x = \frac{i}{N} \int_a^b \bar{\rho}_X \,\mathrm{d}x, \quad i = 0, 1, \ldots, N, \tag{1.6}$$

or

$$(x_i - x_{i-1}) \frac{\rho(x_i) + \rho(x_{i-1})}{2} = \frac{1}{N} \int_a^b \bar{\rho}_X \,\mathrm{d}x, \quad i = 0, 1, \ldots, N. \tag{1.7}$$

Note that the limit mesh X equidistributes $\bar{\rho}_X$ and therefore is, in general, different from the exact equidistributing mesh $\hat{X}$ in (1.1). The existence of X is stated in Theorem 1.1 below. It can also be shown, for sufficiently smooth ρ, that X converges to $\hat{X}$ with a rate of $\mathcal{O}(N^{-2})$ as $N \to \infty$ (see (5.12)).

Let us define

$$\mathcal{M}_N = \left\{ Y \colon y_0 = a < y_1 < \cdots < y_N = b, \frac{(b-a)\rho_-}{N\rho_+} \leqslant y_i - y_{i-1} \leqslant \frac{(b-a)\rho_+}{N\rho_-}, i = 1, \ldots, N \right\}. \tag{1.8}$$

It is not difficult to show that $\mathcal{M}_N$ is a closed and convex subset of $\mathbb{R}^{N+1}$. Moreover, Lemma 2.2 of Section 2 implies that G_N maps $\mathcal{M}_N$ into $\mathcal{M}_N$, i.e.,

$$G_N(\mathcal{M}_N) \subseteq \mathcal{M}_N. \tag{1.9}$$

Let $W^{1,\infty}(a, b)$ and $W^{2,\infty}(a, b)$ be the Sobolev spaces of functions whose first-order and second-order derivatives, respectively, are in $L^\infty(a, b)$. Denote the L^∞-norm by $\|\cdot\|_\infty$. The main result of this paper is given in the following theorem.

THEOREM 1.1 Assume that $\rho \in C[a,b]$ is chosen such that (1.3) holds. Then the following statements hold.

(a) The mapping G_N has at least one fixed point in $\mathcal{M}_N$. In other words, there exists at least one limit mesh satisfying (1.7).
(b) If $\rho \in W^{1,\infty}(a,b)$ then, for sufficiently large N, the mapping G_N has a unique fixed point in $\mathcal{M}_N$ and de Boor's algorithm converges to the limit mesh satisfying (1.7).
(c) If also $\rho \in W^{2,\infty}(a,b)$ then the conclusion in (b) holds for any $N > N_0$, where

$$N_0 \equiv \frac{2(b-a)^2\rho_+}{(\rho_-)^2}\|\rho''\|_\infty + \frac{5(b-a)\rho_+}{(\rho_-)^2}\|\rho'\|_\infty.$$

A very similar result was obtained by Pryce (1989) for the modified de Boor's algorithm using piecewise linear interpolation. In Pryce (1989) the adaptation functions ρ and ρ' are assumed to be Lipschitz continuous in cases (b) and (c), respectively. This condition is the same as that in the above theorem since a function or its derivative is Lipschitz continuous if and only if it is in $W^{1,\infty}(a,b)$ or $W^{2,\infty}(a,b)$, respectively (see, e.g., Evans, 1998).

It needs to be pointed out that the current work is not simply a derivative of Pryce's. Indeed, a key step in Pryce's proof is to show that, in the L^∞-norm, a piecewise linear interpolant is continuous for any $N > 0$ and Lipschitz continuous (with a small Lipschitz constant) for sufficiently large N with respect to the mesh. Unfortunately, this is no longer true for the current situation with piecewise constant interpolation. We avoid this difficulty in the current analysis (and particularly in the proof of Theorem 1.1(a)) by using the L^2-norm for interpolation functions and by the special structure of the piecewise constant interpolation (cf. Lemma 2.1). By considering G_N as a single mapping (instead of a composition of two mappings corresponding to the steps in de Boor's algorithm, as considered in Pryce (1989)), we prove (b) and (c) of Theorem 1.1.

An outline of this paper is as follows. Properties of equidistributing meshes and interpolation error bounds thereon are derived in Section 2. Part (a) of Theorem 1.1 is proved in Section 3, while (b) and (c) are proved in Section 4. In Section 5 numerical results are presented to verify the theoretical findings. Two stopping criteria are also discussed in this section.

2. Properties of equidistributing meshes

In this section we derive several properties of meshes in $\mathcal{M}_N$ and interpolation error estimates thereon. The results are needed to prove Theorem 1.1.

Given a mesh

$$X\colon a = x_0 < x_1 < \cdots < x_N = b, \tag{2.1}$$

we let

$$h_i^X = x_i - x_{i-1}, \quad h_X = \max_i h_i^X. \tag{2.2}$$

The subscript or superscript X is suppressed when no confusion is caused.

Consider piecewise constant and linear interpolation on X. For any continuous function $v(x)$ we define

$$\bar{v}_X|_{(x_{i-1},x_i]} = \frac{v(x_{i-1}) + v(x_i)}{2}, \quad i = 1, \ldots, N, \tag{2.3}$$

$$\hat{v}_X|_{[x_{i-1},x_i]} = v(x_{i-1})\frac{x_i - x}{h_i} + v(x_i)\frac{x - x_{i-1}}{h_i}, \quad i = 1, \ldots, N. \tag{2.4}$$

They can be written in the form

$$\bar{v}_X(x) = \sum_{i=0}^{N} v(x_i)\bar{\phi}_i(x), \quad \hat{v}_X(x) = \sum_{i=0}^{N} v(x_i)\hat{\phi}_i(x), \tag{2.5}$$

where the basis functions are given by

$$\bar{\phi}_i(x) = \begin{cases} \frac{1}{2}, & \text{for } x \in (x_{i-1}, x_{i+1}], \\ 0, & \text{otherwise}, \end{cases} \tag{2.6}$$

$$\hat{\phi}_i(x) = \begin{cases} \frac{x - x_{i-1}}{h_i}, & \text{for } x \in [x_{i-1}, x_i], \\ \frac{x_{i+1} - x}{h_{i+1}}, & \text{for } x \in [x_i, x_{i+1}], \\ 0, & \text{otherwise}. \end{cases} \tag{2.7}$$

LEMMA 2.1 For any continuous function v we have

$$\int_{x_{i-1}}^{x_i} \bar{v}_X \, dx = \int_{x_{i-1}}^{x_i} \hat{v}_X \, dx, \quad i = 1, \ldots, N. \tag{2.8}$$

Proof. The result follows immediately from the definitions (2.3) and (2.4). □

LEMMA 2.2 For any mesh X of N elements, mesh Y that exactly equidistributes $\bar{\rho}_X$ or $\hat{\rho}_X$ satisfies

$$\frac{(b-a)\rho_-}{N\rho_+} \leqslant y_i - y_{i-1} \leqslant \frac{(b-a)\rho_+}{N\rho_-}, \quad i = 1, \ldots, N. \tag{2.9}$$

Proof. The proof is given for the case $\bar{\rho}_X$ only since the same also applies to the case $\hat{\rho}_X$.

We first note that $\bar{\rho}_X$ satisfies (1.3), i.e.,

$$\rho_- \leqslant \bar{\rho}_X(x) \leqslant \rho_+ \quad \forall\, x \in [a, b]. \tag{2.10}$$

Since Y exactly equidistributes $\bar{\rho}_X$, we have

$$\int_{y_{i-1}}^{y_i} \bar{\rho}_X(x) dx = \frac{1}{N}\int_a^b \bar{\rho}_X \, dx, \quad i = 1, \ldots, N. \tag{2.11}$$

Combining (2.10) and (2.11), we have

$$(y_i - y_{i-1})\rho_- \leqslant \int_{y_{i-1}}^{y_i} \bar{\rho}_X(x) dx = \frac{1}{N}\int_a^b \bar{\rho}_X \, dx \leqslant \frac{1}{N}(b-a)\rho_+$$

and

$$(y_i - y_{i-1})\rho_+ \geqslant \int_{y_{i-1}}^{y_i} \bar{\rho}_X(x) dx = \frac{1}{N}\int_a^b \bar{\rho}_X \, dx \geqslant \frac{1}{N}(b-a)\rho_-,$$

which imply (2.9). □

This lemma implies that $G_N(X) \in \mathcal{M}_N$ for any mesh X, and, in particular, that (1.9) holds. Moreover, we need to only consider meshes in $\mathcal{M}_N$ for the convergence analysis.

LEMMA 2.3 For any mesh $X \in \mathcal{M}_N$ and any function $v \in W^{1,\infty}(a,b)$ we have

$$\|\bar{v}_X - v\|_\infty \leqslant \frac{(b-a)\rho_+}{N\rho_-}\|v'\|_\infty, \tag{2.12}$$

$$\|\hat{v}_X - v\|_\infty \leqslant \frac{(b-a)\rho_+}{N\rho_-}\|v'\|_\infty, \tag{2.13}$$

$$\|\hat{v}_X - \bar{v}_X\|_\infty \leqslant \frac{2(b-a)\rho_+}{N\rho_-}\|v'\|_\infty, \tag{2.14}$$

$$\|\hat{v}'_X - v'\|_\infty \to 0 \quad \text{as} \quad N \to \infty. \tag{2.15}$$

Moreover, if $v \in W^{2,\infty}(a,b)$ then we have

$$\|\hat{v}'_X - v'\|_\infty \leqslant \frac{(b-a)\rho_+}{N\rho_-}\|v''\|_\infty. \tag{2.16}$$

Proof. The inequalities (2.12), (2.13) and (2.16) can be deduced from the general interpolation theory for Sobolev spaces (see, e.g., Ciarlet, 1978). The inequality (2.14) follows from (2.12), (2.13) and the triangle inequality.

To prove (2.15) we need the following estimate. For any function $v \in W^{1,\infty}(a,b)$ and for $x \in [x_{i-1}, x_i]$ we have

$$|\hat{v}'_X(x)| = \left|\frac{v(x_i) - v(x_{i-1})}{h_i}\right| = \frac{1}{h_i}\left|\int_{x_{i-1}}^{x_i} v'(s)\mathrm{d}s\right| \leqslant \|v'\|_\infty. \tag{2.17}$$

Note that $W^{2,\infty}(a,b)$ is dense in $W^{1,\infty}(a,b)$. Then, for any $\epsilon > 0$, there exists a function $V \in W^{2,\infty}(a,b)$ such that

$$\|V - v\|_\infty < \frac{\epsilon}{2}, \quad \|V' - v'\|_\infty < \frac{\epsilon}{2}. \tag{2.18}$$

Moreover, we have

$$\begin{aligned}
\|\hat{v}'_X - v'\|_\infty &= \|\hat{v}'_X - \hat{V}'_X + \hat{V}'_X - V' + V' - v'\|_\infty \\
&\leqslant \|\hat{v}'_X - \hat{V}'_X\|_\infty + \|\hat{V}'_X - V'\|_\infty + \|V' - v'\|_\infty \\
&\leqslant \|\hat{v}'_X - \hat{V}'_X\|_\infty + \frac{(b-a)\rho_+}{N\rho_-}\|V''\|_\infty + \|V' - v'\|_\infty \qquad \text{((2.16), replacing } v \text{ by } V) \\
&= \|\widehat{(v - V)}'_X\|_\infty + \frac{(b-a)\rho_+}{N\rho_-}\|V''\|_\infty + \|V' - v'\|_\infty \\
&\leqslant \|v' - V'\|_\infty + \frac{(b-a)\rho_+}{N\rho_-}\|V''\|_\infty + \|V' - v'\|_\infty \quad \text{((2.17), replacing } v \text{ by } v - V) \\
&\leqslant \epsilon + \frac{(b-a)\rho_+}{N\rho_-}\|V''\|_\infty \quad \text{(using (2.18))}.
\end{aligned}$$

Taking the limit as $N \to \infty$ in the above inequality, we get

$$\lim_{N\to\infty} \|\hat{v}'_X - v'\|_\infty \leqslant \epsilon.$$

Letting $\epsilon \to 0$, we obtain (2.15). □

LEMMA 2.4 For any $v \in W^{1,\infty}(a,b)$ and for any two meshes of N elements, X and Y, we have

$$\|\hat{v}_X - \hat{v}_Y\|_\infty \leqslant \|X - Y\|_\infty \max\{\|\hat{v}'_X - v'\|_\infty, \|\hat{v}'_Y - v'\|_\infty\}. \tag{2.19}$$

Proof. The proof is similar to that of Lemma 3.4 in Pryce (1989). Note that

$$\begin{aligned}
\hat{v}_X(x_i) - \hat{v}_Y(x_i) &= v(x_i) - \hat{v}_Y(x_i) \\
&= v(y_i) - \hat{v}_Y(y_i) + \int_{y_i}^{x_i} (v'(s) - \hat{v}'_Y(s))\mathrm{d}s \\
&= \int_{y_i}^{x_i} (v'(s) - \hat{v}'_Y(s))\mathrm{d}s.
\end{aligned}$$

It follows that $|\hat{v}_X(x_i) - \hat{v}_Y(x_i)| \leqslant \|X - Y\|_\infty \|\hat{v}'_Y - v'\|_\infty$. Similarly, $|\hat{v}_X(y_i) - \hat{v}_Y(y_i)| \leqslant \|X - Y\|_\infty \|\hat{v}'_X - v'\|_\infty$. Since $\hat{v}_X - \hat{v}_Y$ is linear between any two mesh points, we obtain

$$\begin{aligned}
\|\hat{v}_X - \hat{v}_Y\|_\infty &\leqslant \max_i\{|\hat{v}_X(x_i) - \hat{v}_Y(x_i)|, |\hat{v}_X(y_i) - \hat{v}_Y(y_i)|\} \\
&\leqslant \|X - Y\|_\infty \max\{\|\hat{v}'_X - v'\|_\infty, \|\hat{v}'_Y - v'\|_\infty\},
\end{aligned}$$

which gives (2.19). □

3. Existence of limit meshes

The main goal of this section is to prove Theorem 1.1(a), i.e., the existence of a limit mesh satisfying (1.7), using Brouwer's fixed-point theorem. Recall that such a limit mesh is a fixed point of the mapping G_N and is different from the exact equidistributing mesh $\hat{X}$ for $\rho(x)$. (Indeed, the existence of $\hat{X}$ does not imply the existence of a limit mesh.) Since $G_N(\mathcal{M}_N) \subseteq \mathcal{M}_N$ and $\mathcal{M}_N$ is a closed and convex subset of $\mathbb{R}^{N+1}$, the existence of a fixed point follows if $G_N \colon \mathcal{M}_N \to \mathcal{M}_N$ is continuous. For this we first need the following lemma.

LEMMA 3.1 For any two meshes X and Y, the meshes $\xi = G_N(X)$ and $\eta = G_N(Y)$ satisfy

$$\|\xi - \eta\|_\infty \leqslant \frac{2\sqrt{(b-a)}}{\rho_-}\|\bar{\rho}_X - \bar{\rho}_Y\|_2, \tag{3.1}$$

where $\|\cdot\|_2$ denotes the L^2-norm and $\bar{\rho}_X$ and $\bar{\rho}_Y$ are the piecewise constant interpolants for ρ on X and Y, respectively. The mapping $\bar{\rho}_X \to \xi$ is thus Lipschitz continuous.

Proof. Since the meshes ξ and η exactly equidistribute functions $\bar{\rho}_X$ and $\bar{\rho}_Y$, respectively, we have

$$\int_a^{\xi_i} \bar{\rho}_X \,\mathrm{d}x = \frac{i}{N}\int_a^b \bar{\rho}_X \,\mathrm{d}x, \quad i = 1, \ldots, N, \tag{3.2}$$

$$\int_a^{\eta_i} \bar{\rho}_Y \,\mathrm{d}x = \frac{i}{N}\int_a^b \bar{\rho}_Y \,\mathrm{d}x, \quad i = 1, \ldots, N. \tag{3.3}$$

Subtracting (3.3) from (3.2), we have

$$\int_a^{\xi_i} \bar{\rho}_X \,\mathrm{d}x - \int_a^{\eta_i} \bar{\rho}_Y \,\mathrm{d}x = \frac{i}{N}\int_a^b (\bar{\rho}_X - \bar{\rho}_Y)\mathrm{d}x$$

or

$$\int_a^{\xi_i} \bar{\rho}_X \,\mathrm{d}x - \int_a^{\eta_i} \bar{\rho}_X \,\mathrm{d}x = \frac{i}{N}\int_a^b (\bar{\rho}_X - \bar{\rho}_Y)\mathrm{d}x + \int_a^{\eta_i} (\bar{\rho}_Y - \bar{\rho}_X)\mathrm{d}x.$$

It follows that

$$\int_{\eta_i}^{\xi_i} \bar{\rho}_X \,\mathrm{d}x = \frac{i}{N}\int_a^b (\bar{\rho}_X - \bar{\rho}_Y)\mathrm{d}x + \int_a^{\eta_i} (\bar{\rho}_Y - \bar{\rho}_X)\mathrm{d}x.$$

Using property (2.10) and the Schwarz inequality, we get

$$|\xi_i - \eta_i|\rho_- \leqslant 2\sqrt{(b-a)}\|\bar{\rho}_X - \bar{\rho}_Y\|_2,$$

which gives (3.1). □

Proof of Theorem 1.1 (a). To prove the continuity of G_N it suffices from Lemma 3.1 to show that the mapping $X \to \bar{\rho}_X$ is continuous in the L^2-norm, that is

$$\|\bar{\rho}_Y - \bar{\rho}_X\|_2 \to 0 \quad \text{as} \quad \|X - Y\|_\infty \to 0. \tag{3.4}$$

(This does not hold in the L^∞-norm.) From (2.5) we have

$$\begin{aligned}
\|\bar{\rho}_Y - \bar{\rho}_X\|_2 &= \left\|\sum_i \rho(y_i)\bar{\phi}_i^Y(x) - \sum_i \rho(x_i)\bar{\phi}_i^X(x)\right\|_2 \\
&\leqslant \left\|\sum_i (\rho(y_i) - \rho(x_i))\bar{\phi}_i^Y(x)\right\|_2 + \left\|\sum_i \rho(x_i)(\bar{\phi}_i^Y(x) - \bar{\phi}_i^X(x))\right\|_2 \\
&\leqslant \sqrt{(b-a)}\max_i |\rho(y_i) - \rho(x_i)| + \rho_+\left(\sum_i \frac{1}{4}(|x_{i-1} - y_{i-1}| + |x_i - y_i|)\right)^{1/2} \\
&\leqslant \sqrt{(b-a)}\max_i |\rho(y_i) - \rho(x_i)| + \rho_+\sqrt{\frac{N}{2}\|X - Y\|_\infty}.
\end{aligned}$$

Since ρ is continuous, the first term in the last inequality approaches zero as $\|X - Y\|_\infty \to 0$. Thus we have (3.4).

By combining (3.4) with Lemma 3.1 we show that the mapping G_N: $\mathcal{M}_N \to \mathcal{M}_N$ is continuous, and so G_N has at least one fixed point by Brouwer's theorem. □

4. Convergence of de Boor's algorithm

The key to proving Theorem 1.1(b) and (c) is to show that G_N is a contraction mapping.

LEMMA 4.1 Suppose that $\rho \in W^{1,\infty}(a,b)$. Then, for any meshes $X, Y \in \mathcal{M}_N$, the meshes $\xi = G_N(X)$ and $\eta = G_N(Y)$ satisfy

$$\|\xi - \eta\|_\infty \leqslant \theta_N \|X - Y\|_\infty, \tag{4.1}$$

where

$$\theta_N = \frac{2(b-a)}{\rho_-} \max\{\|\hat{\rho}'_X - \rho'\|_\infty, \|\hat{\rho}'_Y - \rho'\|_\infty\} + \frac{5(b-a)\rho_+}{N(\rho_-)^2}\|\rho'\|_\infty \tag{4.2}$$

$$\to 0 \quad \text{as} \quad N \to \infty. \tag{4.3}$$

If, further, $\rho \in W^{2,\infty}(a,b)$ then

$$\theta_N \leqslant \frac{2(b-a)^2\rho_+}{N(\rho_-)^2}\|\rho''\|_\infty + \frac{5(b-a)\rho_+}{N(\rho_-)^2}\|\rho'\|_\infty. \tag{4.4}$$

Proof. From (3.2) and (3.3) we have

$$\int_{\eta_i}^{\xi_i} \bar{\rho}_X \, \mathrm{d}x = \frac{i}{N}\int_a^b (\bar{\rho}_X - \bar{\rho}_Y)\mathrm{d}x + \int_a^{\eta_i} (\bar{\rho}_Y - \bar{\rho}_X)\mathrm{d}x$$

$$= \frac{i}{N}\int_a^b (\hat{\rho}_X - \hat{\rho}_Y)\mathrm{d}x + \int_a^{\eta_i} (\bar{\rho}_Y - \bar{\rho}_X)\mathrm{d}x \quad \text{(Lemma 2.1)}. \tag{4.5}$$

For the first term, from Lemma 2.4 we have

$$\left|\frac{i}{N}\int_a^b (\hat{\rho}_X - \hat{\rho}_Y)\mathrm{d}x\right| \leqslant (b-a)\|\hat{\rho}_X - \hat{\rho}_Y\|_\infty$$

$$\leqslant (b-a)\|X - Y\|_\infty \max\{\|\hat{\rho}'_X - \rho'\|_\infty, \|\hat{\rho}'_Y - \rho'\|_\infty\}. \tag{4.6}$$

In the following we estimate the second term in (4.5). Let $(x_{j-1}, x_j]$ and $(y_{k-1}, y_k]$ be the intervals in X and Y containing the point η_i, i.e., $\eta_i \in (x_{j-1}, x_j] and \eta_i \in (y_{k-1}, y_k]$. We consider the two separate cases $j = k$ and $j \neq k$.

(i) Case with $j = k$. In this case $\eta_i \in (x_{j-1}, x_j]$ and $\eta_i \in (y_{j-1}, y_j]$. Then we have

$$\int_a^{\eta_i} (\bar{\rho}_Y - \bar{\rho}_X)\mathrm{d}x = \int_{x_{j-1}}^{\eta_i} (\bar{\rho}_Y - \bar{\rho}_X)\mathrm{d}x + \int_a^{x_{j-1}} (\bar{\rho}_Y - \hat{\rho}_Y)\mathrm{d}x$$

$$- \int_a^{x_{j-1}} (\bar{\rho}_X - \hat{\rho}_X)\mathrm{d}x + \int_a^{x_{j-1}} (\hat{\rho}_Y - \hat{\rho}_X)\mathrm{d}x$$

$$= \int_{x_{j-1}}^{\eta_i} (\bar{\rho}_Y - \bar{\rho}_X)\mathrm{d}x + \int_{y_{j-1}}^{x_{j-1}} (\bar{\rho}_Y - \hat{\rho}_Y)\mathrm{d}x + \int_a^{x_{j-1}} (\hat{\rho}_Y - \hat{\rho}_X)\mathrm{d}x, \tag{4.7}$$

where Lemma 2.1 has been used in the last step.

When $x_{j-1} \geqslant y_{j-1}$, we have $(x_{j-1}, \eta_i) \subset (x_{j-1}, x_j)$ and $(x_{j-1}, \eta_i) \subset (y_{j-1}, y_j)$. Thus we have

$$\begin{aligned}\left|\int_{x_{j-1}}^{\eta_i} (\bar{\rho}_Y - \bar{\rho}_X)\mathrm{d}x\right| &= \left|\int_{x_{j-1}}^{\eta_i} \left(\frac{\rho(y_{j-1}) + \rho(y_j)}{2} - \frac{\rho(x_{j-1}) + \rho(x_j)}{2}\right) \mathrm{d}x\right| \\ &= \left|\int_{x_{j-1}}^{\eta_i} \left(\frac{\rho(y_{j-1}) - \rho(x_{i-1})}{2} + \frac{\rho(y_j) - \rho(x_j)}{2}\right) \mathrm{d}x\right| \\ &\leqslant (x_j - x_{j-1})\|X - Y\|_\infty \|\rho'\|_\infty \\ &\leqslant \frac{(b-a)\rho_+}{N\rho_-}\|X - Y\|_\infty \|\rho'\|_\infty. \end{aligned} \tag{4.8}$$

It follows from (4.7) that

$$\begin{aligned}\left|\int_{a}^{\eta_i} (\bar{\rho}_Y - \bar{\rho}_X)\mathrm{d}x\right| &\leqslant \frac{(b-a)\rho_+}{N\rho_-}\|X - Y\|_\infty \|\rho'\|_\infty + \|X - Y\|_\infty \|\bar{\rho}_Y - \hat{\rho}_Y\|_\infty \\ &\quad + (b-a)\|\hat{\rho}_Y - \hat{\rho}_X\|_\infty \\ &\leqslant \frac{(b-a)\rho_+}{N\rho_-}\|X - Y\|_\infty \|\rho'\|_\infty + \|X - Y\|_\infty \|\bar{\rho}_Y - \hat{\rho}_Y\|_\infty \\ &\quad + (b-a)\|X - Y\|_\infty \max\{\|\hat{\rho}'_X - \rho'\|_\infty, \|\hat{\rho}'_Y - \rho'\|_\infty\}, \end{aligned} \tag{4.9}$$

where we have used Lemma 2.4 in the last step.
On the other hand, when $x_{j-1} \leqslant y_{j-1}$, we rewrite (4.7) as

$$\int_a^{\eta_i} (\bar{\rho}_Y - \bar{\rho}_X)\mathrm{d}x = \int_{y_{j-1}}^{\eta_i} (\bar{\rho}_Y - \bar{\rho}_X)\mathrm{d}x + \int_{x_{j-1}}^{y_{j-1}} (\hat{\rho}_X - \bar{\rho}_X)\mathrm{d}x + \int_a^{y_{j-1}} (\hat{\rho}_Y - \hat{\rho}_X)\mathrm{d}x$$

and have

$$\begin{aligned}\left|\int_{a}^{\eta_i} (\bar{\rho}_Y - \bar{\rho}_X)\mathrm{d}x\right| &\leqslant \frac{(b-a)\rho_+}{N\rho_-}\|X - Y\|_\infty \|\rho'\|_\infty + \|X - Y\|_\infty \|\bar{\rho}_X - \hat{\rho}_X\|_\infty \\ &\quad + (b-a)\|X - Y\|_\infty \max\{\|\hat{\rho}'_X - \rho'\|_\infty, \|\hat{\rho}'_Y - \rho'\|_\infty\}. \end{aligned}$$

Combining this result with (4.9), we have

$$\begin{aligned}\left|\int_{a}^{\eta_i} (\bar{\rho}_Y - \bar{\rho}_X)\mathrm{d}x\right| &\leqslant \frac{(b-a)\rho_+}{N\rho_-}\|X - Y\|_\infty \|\rho'\|_\infty \\ &\quad + \|X - Y\|_\infty \max\{\|\bar{\rho}_X - \hat{\rho}_X\|_\infty, \|\bar{\rho}_Y - \hat{\rho}_Y\|_\infty\} \\ &\quad + (b-a)\|X - Y\|_\infty \max\{\|\hat{\rho}'_X - \rho'\|_\infty, \|\hat{\rho}'_Y - \rho'\|_\infty\}. \end{aligned} \tag{4.10}$$

(ii) Case with $j \neq k$. We first consider the case $j < k$. Then we have

$$y_{k-1} < \eta_i \leqslant x_j \leqslant x_{k-1}, \quad y_j \leqslant y_{k-1} \leqslant \eta_i \leqslant x_j. \tag{4.11}$$

It follows that

$$\begin{aligned}
&\left|\int_a^{\eta_i} (\bar{\rho}_Y - \bar{\rho}_X)\mathrm{d}x\right| \\
&= \left|\int_a^{\eta_i} (\hat{\rho}_Y - \hat{\rho}_X)\mathrm{d}x - \int_a^{\eta_i} (\hat{\rho}_Y - \bar{\rho}_Y)\mathrm{d}x + \int_a^{\eta_i} (\hat{\rho}_X - \bar{\rho}_X)\mathrm{d}x\right| \\
&= \left|\int_a^{\eta_i} (\hat{\rho}_Y - \hat{\rho}_X)\mathrm{d}x - \int_{y_j}^{\eta_i} (\hat{\rho}_Y - \bar{\rho}_Y)\mathrm{d}x + \int_{x_{k-1}}^{\eta_i} (\hat{\rho}_X - \bar{\rho}_X)\mathrm{d}x\right| \quad \text{(Lemma 2.1)} \\
&\leqslant (b-a)\|\hat{\rho}_Y - \hat{\rho}_X\|_\infty + \int_{y_j}^{\eta_i} |\hat{\rho}_Y - \bar{\rho}_Y|\mathrm{d}x + \int_{\eta_i}^{x_{k-1}} |\hat{\rho}_X - \bar{\rho}_X|\mathrm{d}x \\
&\leqslant (b-a)\|\hat{\rho}_Y - \hat{\rho}_X\|_\infty + \int_{y_j}^{x_j} |\hat{\rho}_Y - \bar{\rho}_Y|\mathrm{d}x + \int_{y_{k-1}}^{x_{k-1}} |\hat{\rho}_X - \bar{\rho}_X|\mathrm{d}x \quad \text{(using (4.11))} \\
&\leqslant (b-a)\|\hat{\rho}_Y - \hat{\rho}_X\|_\infty + \|X - Y\|_\infty(\|\hat{\rho}_X - \bar{\rho}_X\|_\infty + \|\hat{\rho}_Y - \bar{\rho}_Y\|_\infty).
\end{aligned}$$

Thus, from Lemma 2.4 we get

$$\begin{aligned}
\left|\int_a^{\eta_i} (\bar{\rho}_Y - \bar{\rho}_X)\mathrm{d}x\right| &= (b-a)\|X - Y\|_\infty \max\{\|\hat{\rho}'_X - \rho'\|_\infty, \|\hat{\rho}'_Y - \rho'\|_\infty\} \\
&\quad + \|X - Y\|_\infty(\|\hat{\rho}_X - \bar{\rho}_X\|_\infty + \|\hat{\rho}_Y - \bar{\rho}_Y\|_\infty).
\end{aligned} \tag{4.12}$$

Similarly, for $k < j$ we have

$$x_k \leqslant x_{j-1} < \eta_i \leqslant y_k, \quad x_{j-1} < \eta_i \leqslant y_k \leqslant y_{j-1}$$

and can show that (4.12) holds.

From (4.10) and (4.12) one can see that, for both cases $j = k$ and $j \neq k$, we have

$$\begin{aligned}
\left|\int_a^{\eta_i} (\bar{\rho}_Y - \bar{\rho}_X)\mathrm{d}x\right| &\leqslant \frac{(b-a)\rho_+}{N\rho_-}\|X - Y\|_\infty\|\rho'\|_\infty \\
&\quad + \|X - Y\|_\infty(\|\bar{\rho}_X - \hat{\rho}_X\|_\infty + \|\bar{\rho}_Y - \hat{\rho}_Y\|_\infty) \\
&\quad + (b-a)\|X - Y\|_\infty \max\{\|\hat{\rho}'_X - \rho'\|_\infty, \|\hat{\rho}'_Y - \rho'\|_\infty\}.
\end{aligned} \tag{4.13}$$

Estimate (4.1) with (4.2) then follows from (2.10), (4.5), (4.6), (4.13) and Lemma 2.3. The limit (4.3) and the estimate (4.4) are consequences of (4.2) combined with (2.15) and (2.16) of Lemma 2.3, respectively. □

Proof of Theorem 1.1(b) *and* (c). From Lemma 4.1, for sufficiently large N, we have $\theta_N < 1$, and so $G_N\colon \mathcal{M}_N \to \mathcal{M}_N$ is a contraction mapping. By the contraction mapping theorem, G_N has a unique fixed point, and de Boor's algorithm converges to the fixed point. Thus Theorem 1.1(b) holds. If, further, $\rho \in W^{2,\infty}(a,b)$ then, from (4.4), $\theta_N < 1$ when $N > N_0$, and so (c) follows. □

5. Numerical examples

In this section we present some numerical results obtained using de Boor's algorithm (denoted by PWC—piecewise constant) and its modified version with piecewise linear interpolation (denoted by PWL). Note that the mesh can be computed exactly in both situations since the integral of the piecewise constant or linear approximation of the adaptation function defines a piecewise linear or quadratic function, respectively. Indeed, the mesh $X^{(k+1)}$ can be computed as

$$x_i^{(k+1)} = x_{j-1}^{(k)} + \frac{2\left(\frac{i}{N}P(b) - P(x_{j-1}^{(k)})\right)}{\rho(x_{j-1}^{(k)}) + \rho(x_j^{(k)})}, \quad i = 1, \ldots, N-1, \tag{5.1}$$

for algorithm PWC (cf. (1.5)) and

$$x_i^{(k+1)} = x_{j-1}^{(k)} + \frac{x_j^{(k)} - x_{j-1}^{(k)}}{\rho(x_j^{(k)}) - \rho(x_{j-1}^{(k)})} \cdot \left(\left(\rho^2(x_{j-1}^{(k)}) + 2\left(\frac{i}{N}P(b) - P(x_{j-1}^{(k)})\right) \frac{\rho(x_j^{(k)}) - \rho(x_{j-1}^{(k)})}{x_j^{(k)} - x_{j-1}^{(k-1)}} \right)^{\frac{1}{2}} - \rho(x_{j-1}^{(k)}) \right),$$
$$i = 1, \ldots, N-1, \tag{5.2}$$

for algorithm PWL, where j is the index satisfying

$$P(x_{j-1}^{(k)}) < \frac{i}{N}P(b) \leqslant P(x_j^{(k)})$$

and

$$P(x_i^{(k)}) = \sum_{j=1}^{i} (x_j^{(k)} - x_{j-1}^{(k)}) \cdot \frac{\rho(x_j^{(k)}) + \rho(x_{j-1}^{(k)})}{2}, \quad i = 0, 1, \ldots, N.$$

The computation for both algorithms is stopped when

$$\|X^{(k+1)} - X^{(k)}\|_\infty \equiv \max_i |x_i^{(k+1)} - x_i^{(k)}| \leqslant \epsilon \tag{5.3}$$

or

$$\max_i Q_{\mathrm{eq},i}^{(k)} \leqslant \kappa, \tag{5.4}$$

or a combination of them. Here ϵ is a prescribed tolerance, $\kappa \geqslant 1$ is a prescribed number close to one and $Q_{\mathrm{eq},i}$ is the so-called equidistribution quality measure (see Huang, 2005) defined as

$$Q_{\mathrm{eq},i}^{(k)} \equiv (x_i^{(k)} - x_{i-1}^{(k)}) \frac{\rho(x_{i-1}^{(k)}) + \rho(x_i^{(k)})}{2} \cdot \frac{N}{\int_a^b \bar{\rho}_{X^{(k)}} \mathrm{d}x}. \tag{5.5}$$

Stopping criterion (5.3) is obvious, and so we only elaborate on (5.4). First, when $\max_i Q_{\mathrm{eq},i}^{(k)} = 1$, we have that $X^{(k)}$ satisfies equation (1.7), and, by uniqueness, it is equal to the limit mesh. In this sense, $\max_i Q_{\text{eq},i}^{(k)}$ measures how closely $X^{(k)}$ satisfies the equidistribution relation (1.7). Moreover, from Lemma 4.1 we have

$$\|X^{(k+1)} - X^{(k)}\|_\infty \leqslant \theta_N \|X^{(k)} - X^{(k-1)}\|_\infty \leqslant \cdots \leqslant \theta_N^k \|X^{(1)} - X^{(0)}\|_\infty \tag{5.6}$$

and

$$\|X^{(k)} - X\|_\infty \leqslant \theta_N^k \|X^{(0)} - X\|_\infty, \tag{5.7}$$

where X denotes the limit mesh. Inequality (5.7) can also be written as

$$X^{(k)} = X + \mathcal{O}(\theta_N^k). \tag{5.8}$$

Using this and (5.5), it is not hard to show that

$$Q_{\text{eq},i}^{(k)} = 1 + \mathcal{O}(\theta_N^k). \tag{5.9}$$

Thus $\max_i Q_{\text{eq},i}^{(k)} - 1$, $\|X^{(k+1)} - X^{(k)}\|_\infty$ and $\|X^{(k)} - X\|_\infty$ all converge to zero at the same order as $k \to \infty$.

We consider an example of the adaptation function in the form

$$\begin{aligned}\rho(x) = 1 + \alpha\,\mathrm{e}^{-\alpha x} &+ R_1(1 - \tanh^2(R_1(x - x_1))) \\ &+ R_2(1 - \tanh^2(R_2(x - x_2))) + R_3(1 - \tanh^2(R_3(x - x_3))), \quad x \in [0, 1].\end{aligned} \tag{5.10}$$

Two sets of parameters are chosen as follows:

$$\rho_1(x)\colon\ \alpha = 0, \quad R_1 = 20, \quad x_1 = 0.15, \quad R_2 = 30, \quad x_2 = 0.5, \quad R_3 = 10, \quad x_3 = 0.75,$$

$$\rho_2(x)\colon\ \alpha = 500, \quad R_1 = 20, \quad x_1 = 0.25, \quad R_2 = 120, \quad x_2 = 0.5, \quad R_3 = 15, \quad x_3 = 0.75.$$

The adaptation function $\rho_1(x)$ has competing localized structures located at 0.15, 0.5 and 0.75, while $\rho_2(x)$ has a sharp boundary layer at $x = 0$ together with a salient localized structure and two relatively small-scale structures. The function $\rho_2(x)$ is rougher than $\rho_1(x)$, and we expect that the algorithm requires a larger number of mesh points to converge for ρ_2 than for ρ_1.

The numerical results are shown in Tables 1 and 2 and in Figs 1–3. From these results we can make the following observations.

TABLE 1 *Results obtained for* $\rho_1(x)$. Iter *is the number of iterations required to reach* (5.4) *with* $\kappa = 1.0001$, F *indicates that* (5.4) *is not reached in the maximal allowed number of iterations (set to be* 10,000*), X denotes the convergent mesh and $\hat{X}$ is the exact equidistributing mesh for ρ_1, which is computed using Newton's iteration*

N		11	21	41	81	161	321	641	1281
Iter	PWC	F	28	8	7	6	4	3	2
	PWL	F	F	F	12	5	3	2	2
$\|X - \hat{X}\|_\infty$	PWC		4.36×10^{-2}	1.99×10^{-2}	8.61×10^{-3}	2.56×10^{-3}	7.29×10^{-4}	1.86×10^{-4}	4.67×10^{-5}
	PWL				8.61×10^{-3}	2.56×10^{-3}	7.27×10^{-4}	1.87×10^{-4}	4.67×10^{-5}

TABLE 2 *Results obtained for* $\rho_2(x)$. Iter *is the number of iterations required to reach* (5.4) *with* $\kappa = 1.0001$, F *indicates that* (5.4) *is not reached in the maximal allowed number of iterations (set to be* 10,000*), X denotes the convergent mesh and* $\hat{X}$ *is the exact equidistributing mesh for* ρ_2*, which is computed using Newton's iteration*

N		41	81	161	321	641	1281
Iter	PWC	F	14	12	9	8	6
	PWL	F	F	F	F	14	6
$\\|X - \hat{X}\\|_\infty$	PWC		5.33×10^{-2}	2.37×10^{-2}	8.61×10^{-3}	3.35×10^{-3}	1.03×10^{-3}
	PWL					3.35×10^{-3}	1.03×10^{-3}

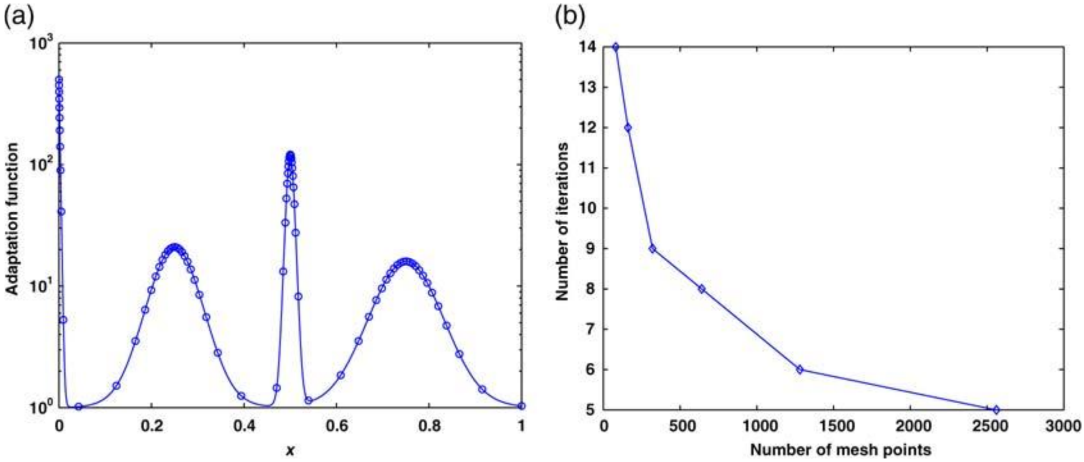

FIG. 1. Results obtained for the adaptation function $\rho_2(x)$ using de Boor's algorithm (PWC) with $\kappa = 1.0001$. (a) The mesh points of the limit mesh ($N = 81$) are shown on the graph of $\rho_2(x)$. (b) The number of iterations required to reach (5.4) is plotted against the number of mesh points.

(i) In general, PWC converges faster than PWL. Tables 1 and 2 show that the number of iterations required to reach (5.4) is consistently smaller with PWC than with PWL. This can also be seen in Figs 2 and 3, which show that θ_N (the contraction constant; cf. Lemma 4.1) is smaller with PWC than with PWL. Otherwise, the algorithms behave similarly. The reason why PWC is faster than PWL is not obvious from either our analysis or that of Pryce (1989).

(ii) Both algorithms converge faster for larger N (cf. Tables 1 and 2 and Fig. 1(b)). This is consistent with Lemma 4.1, which shows that $\theta_N \to 0$ as $N \to \infty$.

(iii) Figures 2 and 3 clearly show that the convergence of $\max_i Q_{\mathrm{eq},i}^{(k)} - 1$ and $\|X^{(k+1)} - X^{(k)}\|_\infty$ behaves as in (5.9) and (5.6). This demonstrates that both (5.3) and (5.4) are effective stopping criteria.

(iv) The values of N_0 defined in Theorem 1.1(c) corresponding to $\rho_1(x)$ and $\rho_2(x)$ in Tables 1 and 2 are $N_0 \approx 3 \times 10^6$ and $N_0 \approx 1 \times 10^{11}$, respectively. Thus, this estimate that is needed in the general theory is very conservative, and de Boor's algorithm converges for a much smaller number of mesh points.

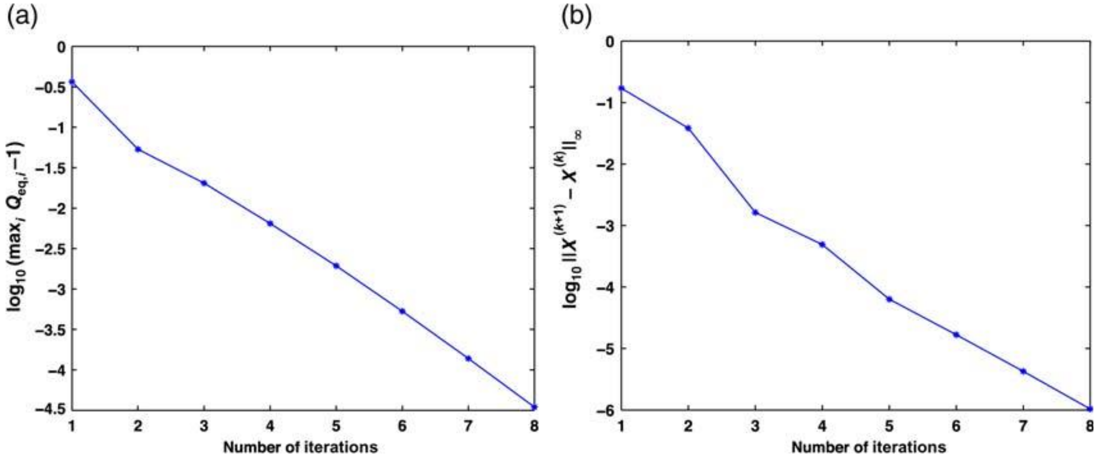

FIG. 2. Results obtained for the adaptation function $\rho_2(x)$ using de Boor's algorithm (PWC) with $N = 641$ and $\kappa = 1.0001$. (a) $\log_{10}(\max_i Q_{\mathrm{eq},i} - 1)$ is plotted against the iteration number k. (b) $\log_{10} \|X^{(k+1)} - X^{(k)}\|_\infty$ is plotted against the iteration number k. The slope of both curves is approximately -0.60, which indicates that $\theta_N \approx 0.2512$.

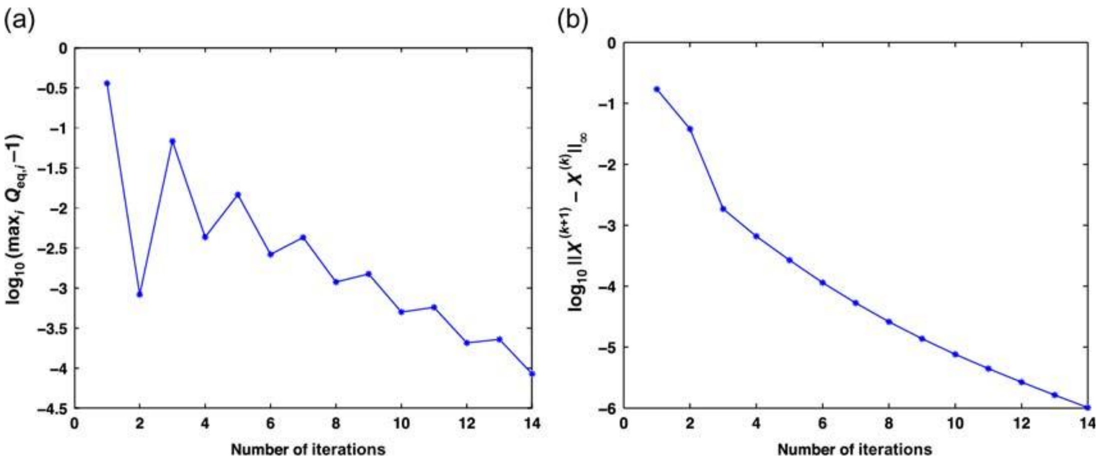

FIG. 3. Results obtained for the adaptation function $\rho_2(x)$ using the modified de Boor's algorithm (PWL) with $N = 641$ and $\kappa = 1.0001$. (a) $\log_{10}(\max_i Q_{\mathrm{eq},i} - 1)$ is plotted against the iteration number k. (b) $\log_{10} \|X^{(k+1)} - X^{(k)}\|_\infty$ is plotted against the iteration number k. The slope of both curves is approximately -0.20, which indicates that $\theta_N \approx 0.6310$.

(v) The converged meshes obtained with both algorithms are almost the same (cf. Tables 1 and 2). This is not surprising since the limit meshes for PWC and PWL satisfy the same equation (1.7). Moreover, the numerical results in Tables 1 and 2 show that the difference between the convergent mesh and the exact equidistributing mesh decreases by the rate $\mathcal{O}(1/N^2)$ as $N \to \infty$. This can be explained by examining the accuracy of the limit mesh. Indeed, by subtracting (1.6) from (1.1), we have

$$\int_a^{\hat{x}_i} \rho(x)\mathrm{d}x - \int_a^{x_i} \bar{\rho}_X(x)\mathrm{d}x = \frac{i}{N}\left(\int_a^b \rho(x)\mathrm{d}x - \int_a^b \bar{\rho}_X(x)\mathrm{d}x\right).$$

Applying Lemma 2.1, we get

$$\int_a^{\hat{x}_i} \rho(x)\mathrm{d}x - \int_a^{x_i} \hat{\rho}_X(x)\mathrm{d}x = \frac{i}{N}\left(\int_a^b \rho(x)\mathrm{d}x - \int_a^b \hat{\rho}_X(x)\mathrm{d}x\right)$$

or

$$\int_{x_i}^{\hat{x}_i} \rho(x)\mathrm{d}x = \frac{i}{N}\int_a^b (\rho(x) - \hat{\rho}_X(x))\mathrm{d}x - \int_a^{x_i} (\hat{\rho}_X(x) - \rho(x))\mathrm{d}x. \quad (5.11)$$

It is not difficult to show (cf. Lemma 2.3) that, when $\rho \in W^{2,\infty}(a, b)$, we have

$$\|\rho - \hat{\rho}_X\|_\infty \leqslant \frac{C}{N^2}\|\rho''\|_\infty$$

for some constant C. Thus, from (5.11) we have

$$\|X - \hat{X}\|_\infty \leqslant \frac{2(b-a)C}{N^2\rho_-}\|\rho''\|_\infty. \quad (5.12)$$

Funding

Natural Sciences and Engineering Research Council of Canada (OGP-0008781 to X.X., A8781 to R.D.R.); National Science Foundation of U.S.A. (DMS-0410545, DMS-0712935 to W.H.).

REFERENCES

BABUŠKA, I. & RHEINBOLDT, W. C. (1978) A posteriori error estimates for the finite element method. *Int. J. Numer. Methods Eng.*, **12**, 1597–1615.

BECKETT, G. & MACKENZIE, J. A. (2000) Convergence analysis of finite-difference approximations on equidistributed grids to a singularly perturbed boundary value problem. *Appl. Numer. Math.* **35**, 87–109.

BECKETT, G. & MACKENZIE, J. A. (2001) On a uniformly accurate finite difference approximation of a singularly perturbed reaction–diffusion problem using grid equidistribution. *J. Comput. Appl. Math.*, **131**, 381–405.

BURCHARD, H. G. (1974) Splines (with optimal knots) are better. *Appl. Anal.*, **3**, 309–319.

CHEN, L., SUN, P. & XU, J. C. (2007) Optimal anisotropic meshes for minimizing interpolation errors in L^p-norm. *Math. Comput.*, **76**, 179–204.

CIARLET, P. G. (1978) *The Finite Element Method for Elliptic Problems*. Amsterdam: North-Holland.

DE BOOR, C. (1973) Good approximation by splines with variable knots. *Spline Functions and Approximation Theory* (A. Meir & A. Sharma eds). Basel: Birkhäuser, pp. 57–73.

DE BOOR, C. (1974) Good approximation by splines with variables knots II. *Conference on the Numerical Solution of Differential Equations*, Dundee, Scotland, 1973 (G. A. Watson ed.). Lecture Notes in Mathematics, vol. 363. Berlin: Springer, pp. 12–20.

DODSON, D. S. (1972) Optimal order approximation by polynomial spline functions. *Ph.D. Thesis*, Purdue University.

EVANS, L. C. (1998) *Partial Differential Equations*. Graduate Studies in Mathematics, vol. 19. Providence, RI: American Mathematical Society.

HUANG, W. (2005) Measuring mesh qualities and application to variational mesh adaptation. *SIAM J. Sci. Comput.*, **26**, 1643–1666.

HUANG, W., REN, Y. & RUSSELL, R. D. (1994) Moving mesh partial differential equations (MMPDEs) based upon the equidistribution principle. *SIAM J. Numer. Anal.*, **31**, 709–730.

HUANG, W. & SUN, W. (2003) Variational mesh adaptation II: error estimates and monitor functions. *J. Comput. Phys.*, **184**, 619–648.

KOPTEVA, N. & STYNES, M. (2001) A robust adaptive method for a quasi-linear one-dimensional convection–diffusion problem. *SIAM J. Numer. Anal.*, **39**, 1446–1467.

LINSS, T. (2001) Uniform pointwise convergence of finite difference schemes using grid equidistribution. *Computing*, **66**, 27–39.

MACKENZIE, J. (1999) Uniform convergence analysis of an upwind finite-difference approximation of a convection–diffusion boundary value problem on an adaptive grid. *IMA J. Numer. Anal.*, **19**, 233–249.

PEREYRA, V. & SEWELL, E. G. (1975) Mesh selection for discrete solution of boundary problems in ordinary differential equations. *Numer. Math.*, **23**, 261–268.

PRYCE, J. D. (1989) On the convergence of iterated remeshing. *IMA J. Numer. Anal.*, **9**, 315–335.

QIU, Y. & SLOAN, D. M. (1999) Analysis of difference approximations to a singularly perturbed two-point boundary value problem on an adaptively generated grid. *J. Comput. Appl. Math.*, **101**, 1–25.

QIU, Y., SLOAN, D. M. & TANG, T. (2000) Numerical solution of a singularly perturbed two-point boundary value problem using equidistribution: analysis of convergence. *J. Comput. Appl. Math.*, **116**, 121–143.

RICE, J. R. (1969) On the degree of convergence of nonlinear spline approximation. *Approximations with Special Emphasis on Spline Functions* (I. J. Schoenberg ed.). New York: Academic Press, pp. 349–365.

RUSSELL, R. D. & CHRISTIANSEN, J. (1978) Adaptive mesh selection strategies for solving boundary value problems. *SIAM J. Numer. Anal.*, **15**, 59–80.

SACKS, J. & YLVISAKER, D. (1966) Designs for regression problems with corrected errors. *Ann. Math. Stat.*, **37**, 66–89.

SACKS, J. & YLVISAKER, D. (1968) Designs for regression problems with corrected errors; many parameters. *Ann. Math. Stat.*, **39**, 49–69.

SACKS, J. & YLVISAKER, D. (1970) Designs for regression problems with corrected errors III. *Ann. Math. Stat.*, **41**, 2057–2074.

WHITE JR, A. B. (1979) On selection of equidistributing meshes for two-point boundary-value problems. *SIAM J. Numer. Anal.*, **16**, 472–502.